JOURNAL OF MATERIALS SCIENCE 30 (1995) 4567–4583

Structure of round-shaped methylnaphthalene-derived mesophase pitch-based carbon fibres prepared by spinning through a Y-shaped die hole

F. FORTIN, S.H. YOON, Y. KORAI, I. MOCHIDA
Institute of Advanced Material Study, Kyushu University 86 Kasuga, Fukuoka 816, Japan

Structures of as-spun, stabilized, carbonized and graphitized fibres prepared by spinning a methylnaphthalene-derived mesophase pitch through a Y-shaped die hole at 295 °C, was examined by combining optical, scanning electron and transmission electron microscopy from the macro- and microscopic view points. The prepared round-shaped fibre spun through a Y-shaped spinning die hole at 295 °C exhibited excellent tensile and compressive strengths of 410 and 70 Kg mm^{-2}, respectively, after graphitization at 2500 °C. The stabilized fibre consisted of densely packed anisotropic domains in very random alignment, of which transverse domains and longitudinal features appeared as bent, multi-bent and looped, and endless thin stripes, respectively. The size of domain in the transverse section ranged above 100 nm in length and below 100 nm in thickness, respectively. Further heat treatment (carbonization and graphitization) slightly reduced the dimension and deformed the shape of domains to shrink and to have more sharp edges at their bends according to the graphitic growth; however, the shapes and distribution of domains in transverse section were basically unchanged. High-resolution SEM and TEM observations of the domain confirmed the existence of smaller units of graphitic layers in their assemblies which were more closely arranged in the domain. Such a sub-unit was defined as a micro-domain. TEM revealed that the micro-domain was composed of more than one unit of graphitic layers in the graphitized fibre. Most of them were around 10 nm thick and 10–100 nm long. The thickness of micro-domains was observed to be smaller than the value of $L_{c(0\,0\,2)}$, 23 nm, in the same graphitized fibre. Micro-domains have not yet been identified in the stabilized fibre, while TEM suggested some stackings of hexagonal planes. A number of voids (micro- and meso-voids) up to 40 nm diameter were formed at the intra- or inter-domain locations, due to the graphitic shrinkage and evolution of volatile matter by the heat treatments. Micro-voids of around 5 nm diameter were formed within a domain. The better mechanical performances of the present fibre spun through a Y-shaped die hole were ascribed to the homogeneous distribution of looped or bent domains in the transverse section (random nature of transverse alignment). Such a random alignment may also lead to the least number of macro-voids and cracks in the fibril.

1. Introduction

Mesophase pitch-based carbon fibres (MPCFs) are recognized as a very promising material for the coming century owing to their characteristic properties (high electric and thermal conductivity) in addition to their excellent tensile properties [1, 2]. A much higher Young's modulus and thermal conductivity compared to those of the PAN-based fibres are easily obtained at a lower graphitization temperature around 2500 °C [3, 4]. The liquid crystal natures of the mesophase pitches with highly ordered alignments of planar mesogen molecules provide a high preferred orientation of the graphitic layers along the fibre axis [5–9].

However, there still remain important problems to be solved for broader applications [10, 11]. So far, as compared to PAN-based carbon fibres, MPCFs are still subject to high production costs in spite of the lower price of pitch precursor, and their compressive strength is unsatisfactory. Because the physical properties of carbon fibres strongly depend on their alignment and structure, further research is needed to clarify the structure and its relation to the performance of the pitch-based carbon fibres [12–14].

It is well known that a number of defects (voids and cracks) in the pitch-based carbon fibres basically define their performances. For example, the open wedge often found in the typical radial transverse alignment is believed to be a fatal factor in deteriorating fibre performance [15].

Recently, we found that round-shaped fibres could be obtained by a high-temperature melt-spinning

0022–2461

regardless of the shape of the spinning die hole [16]. After graphitization, the round-shaped fibre which was spun at 295 °C through a Y-shaped die hole, showed neither macro-voids nor cracks, exhibiting much improved mechanical properties over those of fibres spun from the same pitch through a round-shaped die hole [16–18]. The shapes of the spinning die hole which are expected to define the flow properties of molten melt in the capillary have been reported to be very influential on the transverse alignment and mechanical properties of the resulting carbon fibres [9, 16–18]. The die swell at the outlet of the die hole gives a round shape by relaxing the flow defined by the die hole, and influencing transverse alignment at the same time.

In the present work, we carefully examined the microscopic structure of particular mesophase pitch-based carbon fibres which were prepared from a methylnaphthalene-derived mesophase pitch by spinning through a Y-shaped die hole at a series of temperatures, to control the transverse shape and alignment. The structure in the transverse sections of the resultant fibres was examined by observations under polarized optical (OM), scanning and transmission electron (SEM and TEM) microscopes. Thin-sectioned fibre along its axis was also examined in detail under the OM and TEM.

There have been many research studies into the structure of carbon fibres using transmission electron microscopy [12, 13, 19]. Unfortunately, commercially available fibres were used, and hence it cannot be revealed how the precursor pitch or preparation conditions influence the structure and properties of a series of fibres nor how the heat treatment from stabilization to graphitization changes the structure. Furthermore, microtoming is believed to cause deformation of the structure. Hence, a comparison of as-spun, stabilized, carbonized and graphitized fibres is very essential for producing the exact structure and changes of the mesophase pitch-based carbon fibre.

The relationships between structure and properties of the fibres is briefly discussed.

2. Experimental procedure

2.1. Materials

Table I shows some properties of the mesophase pitch used in the present study. The mesophase pitch was prepared by Mitsubishi Gas Chemical Company from methylnaphthalene using HF/BF_3 as a catalyst [20].

TABLE I Some analytical properties of methylnaphthalene pitch prepared using HF/BF_3 as a catalyst

Softening point (°C)	Anisotropic content (vol. %)	Solubility (wt %)			H/C	F_a
		BS	BI–PS	PI (QI)		
205	100	52	10	33 (29)	0.69	0.86

2.2. Spinning of mesophase pitch

Methylnaphthalene pitch was spun under a nitrogen pressure through a Y-shaped spinning die hole. The dimensions and a schematic picture of the spinning apparatus are illustrated in Fig. 1. Spinning conditions are detailed in Table II.

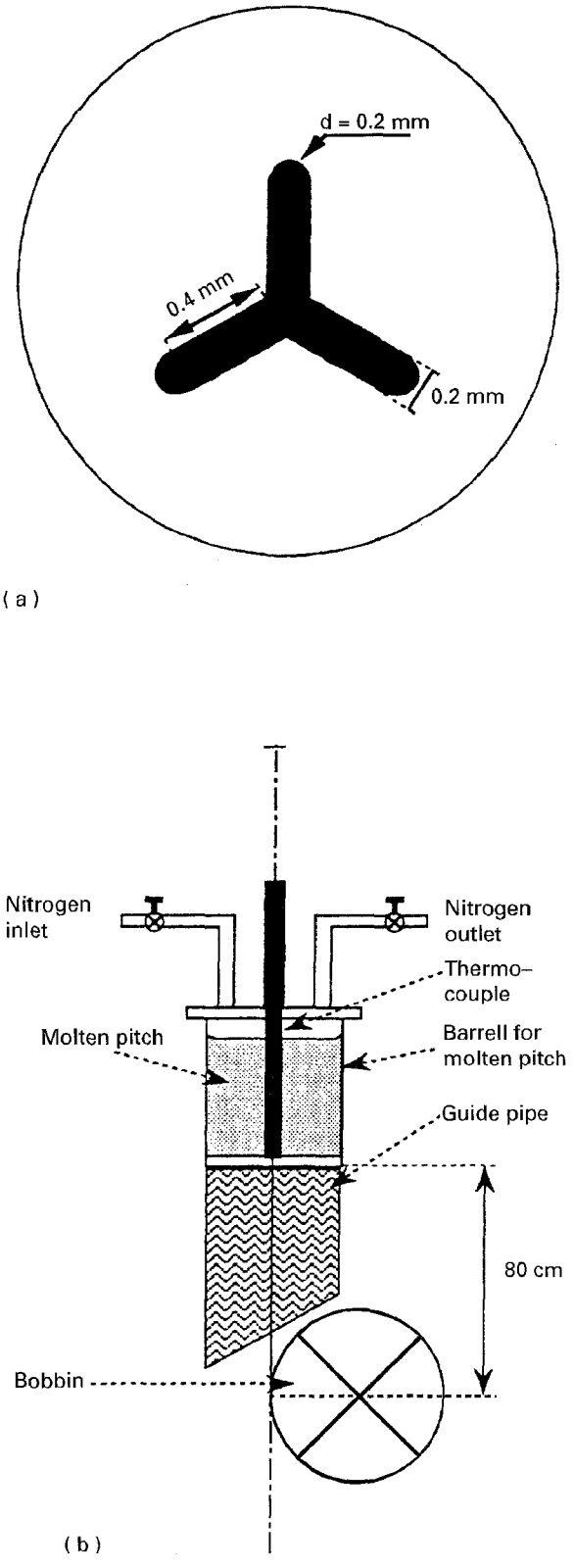

Figure 1 Dimensions of the Y-shaped die hole and spinning apparatus.

TABLE II Spinning temperatures and conditions

Nozzle	Spinning temperature (°C)	Pressure ($kg\,cm^{-2}$)	Extrudate ($mg\,min^{-1}$)	Spinning rate ($m\,min^{-1}$)
Circular	295	1.0	100	800
Y	275	0.5	100	800
	285	0.2	100	800
	295	0.1	100	800

2.3. Stabilization of pitch fibres

The oxidative stabilization of pitch fibres was performed in air at 270 °C for 20 min at a heating rate of 5 °C min^{-1}.

2.4. Carbonization and graphitization of stabilized fibres

Stabilized fibres were carbonized in an argon atmosphere at 1300 °C for 1 h at a heating rate of 10 °C min^{-1}. Carbon fibres were further graphitized at 2500 °C without soaking at a heating rate of 100 °C min^{-1}.

2.5. Characterization of stabilized, carbonized and graphitized fibres

Three complementary techniques of microscopy were coupled to investigate the structure of fibres. The transverse sections of carbonized fibres were examined under a scanning electron microscope (Jeol JSM-5400). Ultra-thin sections (50–80 nm thick) of transverse and longitudinal sections of fibres were obtained by ultramicrotomy (Leica Ultracut S), using a diamond knife, and observed under TEM (Jeol 100CX). Embedded blocks after thin sectioning were directly used for observation under a polarized-light optical microscope (Olympus B061). The transverse sections of all stabilized fibres and the longitudinal section of the stabilized fibre which was spun at 295 °C, were observed under a polarized optical microscope and TEM using the 0 0 2 dark-field mode. The longitudinal and the transverse sections of the graphitized fibre which was spun at 295 °C were observed under TEM using bright-field, 0 0 2 dark-field and lattice fringe modes.

The degree of preferred orientation along the fibre axis was calculated from the full width at half maximum (FWHM) of the (0 0 2) diffraction profile of a fibre bundle, according to the Gakushin method, using a wide-angle X-ray diffractometer with an attachment for fibre samples (Rigaku Geiflex) [21]. $L_{c(0\,0\,2)}$, the height of a crystallite, was measured according to the method defined by the Japanese Society for Promotion of Science [22].

Tensile strength, Young's modulus and strain to break were measured at room temperature using mono-filaments according to the procedure defined in the Japanese Industrial Standard (JIS R-7601), using an Instron-type tensile testing machine (Instron 4200 series) with a crosshead speed of 0.5 mm min^{-1} [23]. Compressive strength was measured by a conventional method which was often used for the composites [24]. Experimental details about measurements of transverse-section area and mechanical properties were described in a previous paper [18]. In all, 16 samples were measured and their properties were averaged; fair reproducibility was reported in a previous paper [18, 23].

3. Results

3.1. Detailed structure of a stabilized round-shaped fibre

Fig. 2 shows the TEM lattice fringe image of the longitudinal section of the stabilized fibre spun at 295 °C. Although the molecular organization is low at this stage, definite stacks of polyaromatic planes were observed (see arrows). Such stack units were aligned more or less in the same direction by the spinning process.

Fig. 3, which compares the alignment of the transverse-section to that of the longitudinal section at different scales, provides some important information concerning the three-dimensional structure of the fibre. Fig. 3a and d are the corresponding 0 0 2 dark-field images. The random character of the domain units in the transverse section are well recognized. The bright units in the transverse section were observed as straight elongated domains without discontinuity in the longitudinal section, as illustrated in Fig. 3a. Domains over 30 μm length can be observed along the fibre axis in Fig. 3d. The extinct lines between two elongated bright domains corresponded to the extinct domains in the transverse section. Thus a domain is expected to be elongated along the fibre axis, maintaining the shape observed in the transverse section. The fibril units formed by cutting the transverse domain along the fibre axis reflected the parallel alignment of aromatic planes. Fig. 3b and c, and e and f are higher magnifications of Fig. 3a and d, respectively. In the transverse section, the domains showed rather irregular shapes. Many domains carried some bent and loop-shaped parts. The domain size in the transverse section ranged above 100 nm and below 100 nm in their length and thickness, respectively. The longitudinal section again showed bright and dark stripes which basically run along the fibre axis.

Fig. 4 exhibits a longitudinal section of its whole diameter (11 μm) (see arrows). The thickness of the fibrils (elongated bright stripes) was estimated to lie in the range 20–200 nm. These elongated stripes numbered 55. Some lines running east to west may be induced during microtoming with the diamond knife.

3.2. Detailed structure of a graphitized round-shaped fibre

Fig. 5a–c are scanning electron micrographs of the transverse sections of graphitized fibres, which were spun at 285, 290 and 295 °C, respectively. The influences of spinning temperature on the shape and

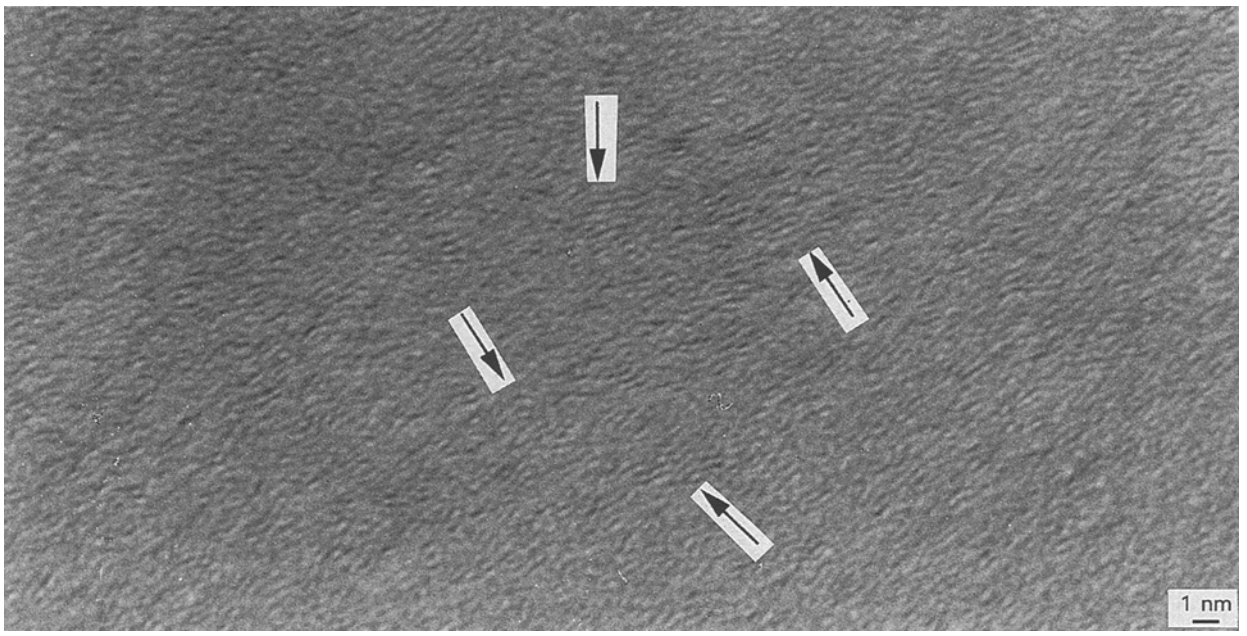

Figure 2 TEM lattice fringe image of a longitudinal section in the round transverse shaped stabilized fibre spun at 295 °C.

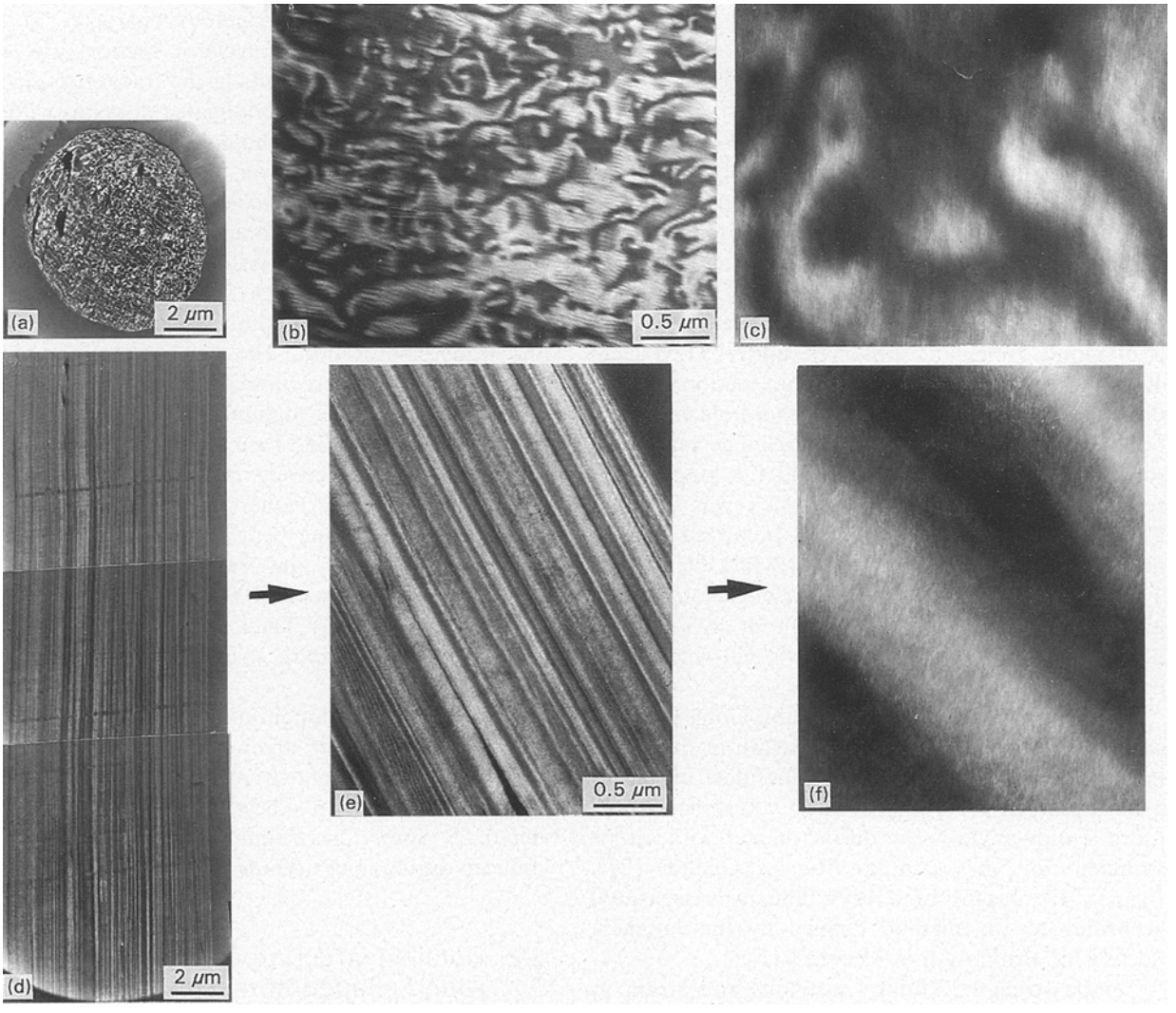

Figure 3 Comparison of the alignment of transverse section and longitudinal section (round-shaped stabilized fibre spun at 295 °C). (a–c) TEM 0 0 2 dark-field images of the transverse section at different scales. (d–f) TEM 0 0 2 dark-field images of the longitudinal section at different scales.

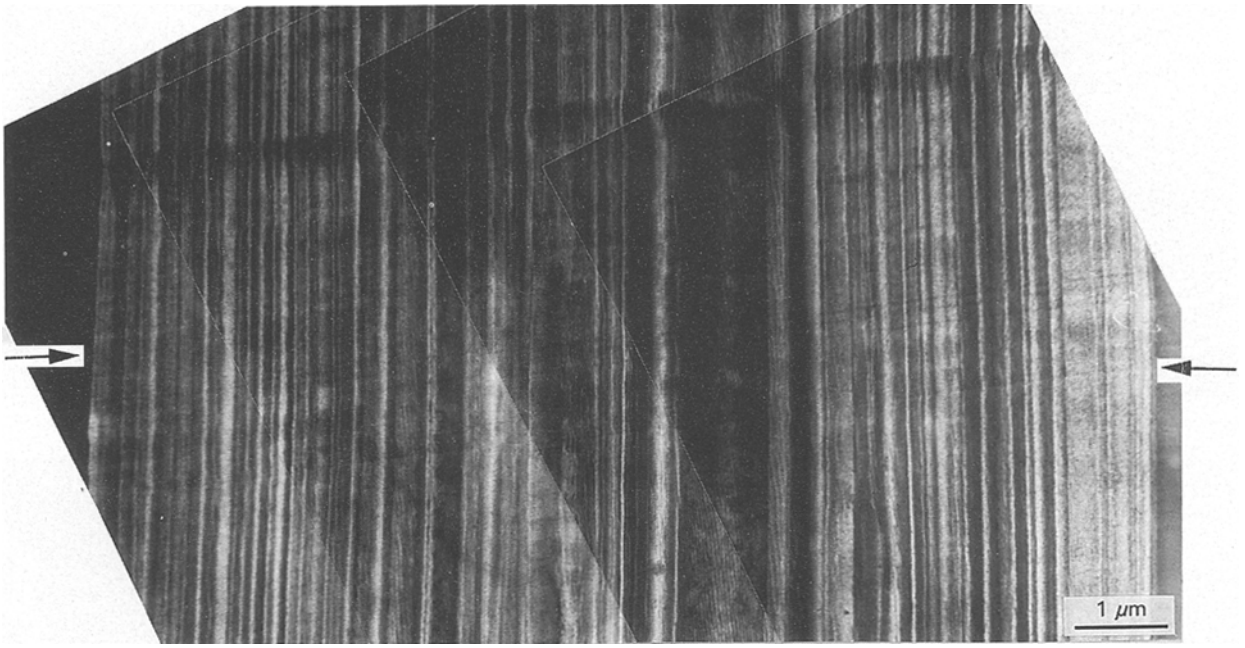

Figure 4 TEM 0 0 2 dark field montage of the longitudinal section of one fibre.

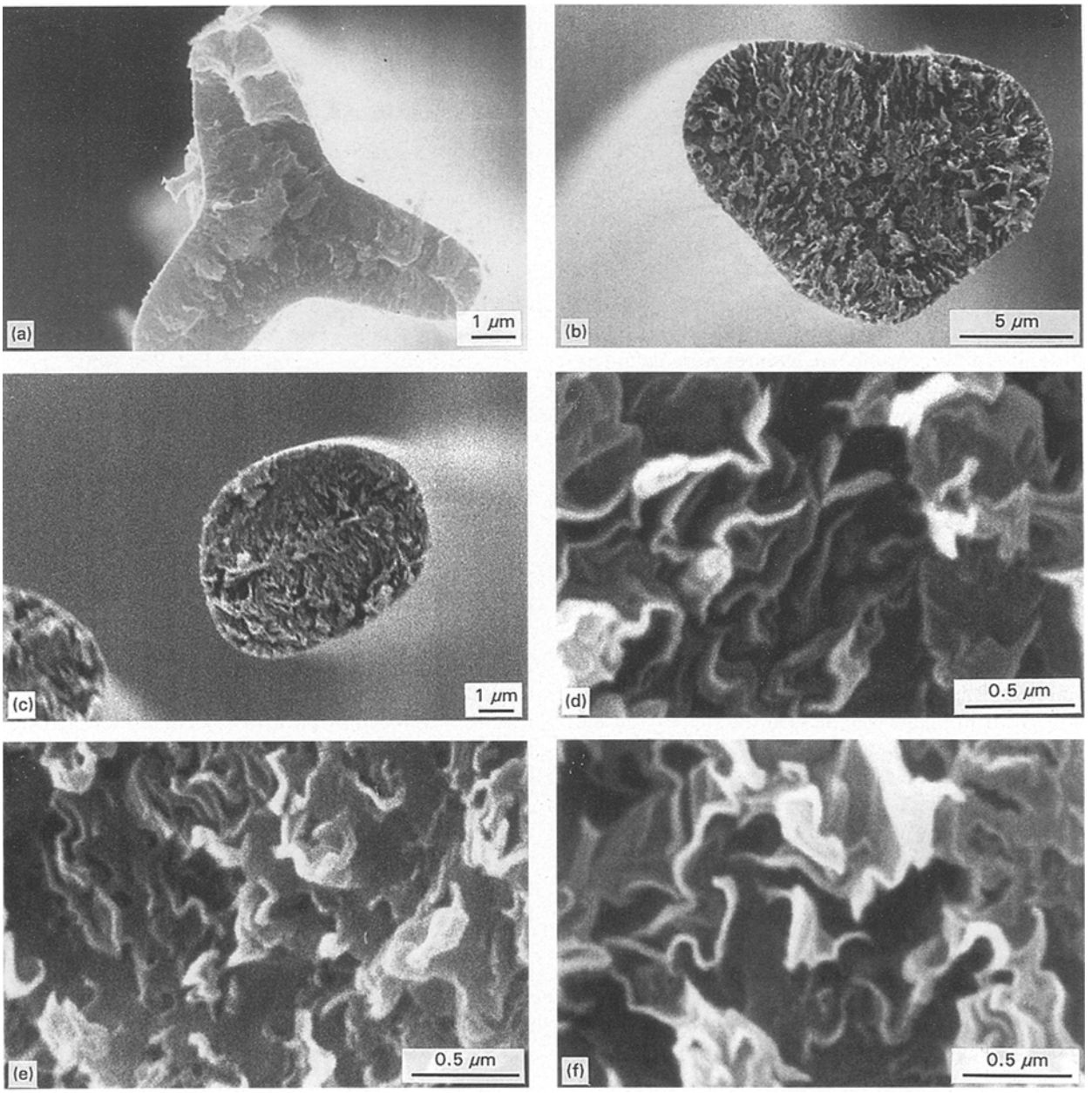

Figure 5 Scanning electron micrographs of the transverse sections of graphitized fibres spun at (a, d) 275 °C, (b, e) 285 °C, (c, f) 295 °C.

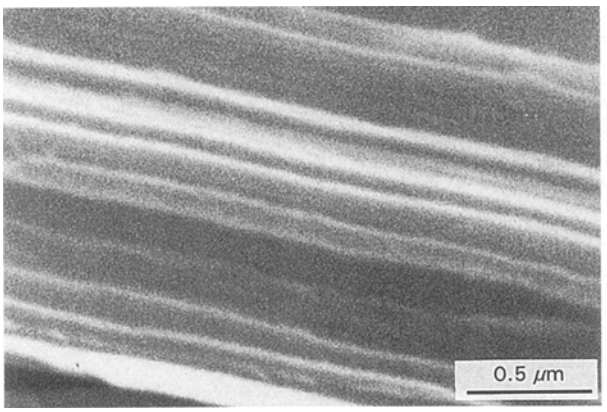

Figure 6 Scanning electron micrograph of the longitudinal section of the graphitized fibre spun at 295 °C.

alignment were well illustrated in the graphitized fibre, as observed in the stabilized fibre in the previous section. Fig. 5d–f are magnified images of their transverse sections. Although domains of complicated shapes with various dimensions were easily identified, their shapes are definitely different from those of the stabilized fibre in their thickness. In the longitudinal section, elongated fibrils in the form of stripes are also visualized by SEM, as shown in Fig. 6.

Fig. 7 shows higher magnification SEM images of the transverse section in the graphitized fibre spun at 295 °C. Fig. 7a and b show the outer and the inner areas of the fibre, respectively. The looped and multi-bent shapes of domains were well observed in both areas.

Such domains were found to be composed of some sub-units, micro-domains, which were not detected in the stabilized fibre. Some line features were definitely identified inside the micro-domain.

Fig. 8a and b show TEM bright-field images of the longitudinal and transverse sections of the graphitized round-shaped fibre, respectively. The damage which was created during microtoming by the diamond knife should be noted. Such damage may introduce changes in the structure. However, some parts of the sections appear to be almost free from damage. Fig. 8c and d exhibit the two orthogonal 0 0 2 dark-field images of the transverse section of Fig. 8b. Both photographs show a homogeneous distribution of bright dots, which confirms the random alignment. In particular, the bright-field image well defined the shapes and the shape distribution of domain units comparable to those in the dark-field images.

The size and shape of the domain units were identified more definitely under larger magnification. Fig. 9a and b show higher magnification 0 0 2 dark-field images of longitudinal and transverse sections, respectively. The magnification is the same as in Fig. 3c and g, hence, the change in the domain size and shape from the stabilized fibre to the graphitized one can be interestingly compared. In the longitudinal section of the graphitized fibre (see Fig. 9a), elongated domains were well visualized. However, they did not appear as straight lines but rather as a discontinuous line-up of smaller elongated domains. Such a discontinuity may

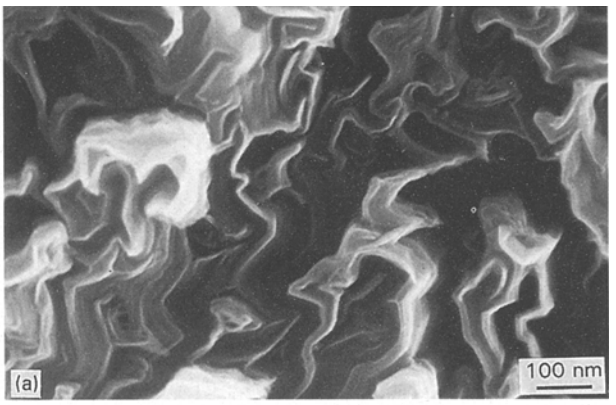

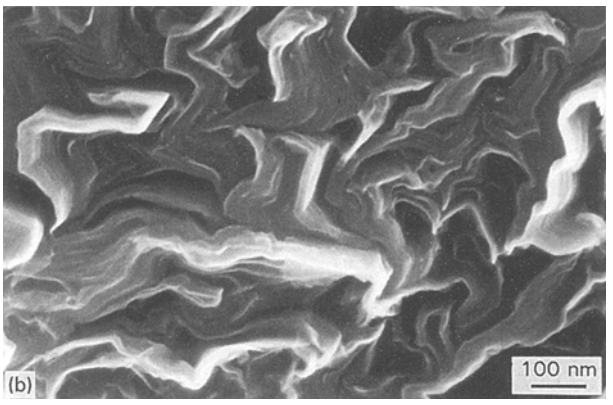

Figure 7 High-resolution scanning electron micrographs of the transverse section of graphitized fibre spun at 295 °C. (a) Outer area, (b) inner area.

be created by the microtoming because the scanning electron micrograph of the same fibre did not show such a discontinuity (see Fig. 6).

In the transverse-section (see Fig. 9b), white spots which represent the crystalline regions were detected. The largest bright spot was ~ 300 nm (arrowed). The density of the bright dots was much lower in the transverse section of the graphitized fibre (Fig. 9b) than that of the stabilized fibre (Fig. 3e), indicating the formation of many defects, major parts of which were caused by the microtoming. The damage induced by the diamond knife can break domains, and forced them to lie flat to the grid.

Fig. 10 shows a higher magnification bright-field image of the transverse section. The shape and size of domains which consisted of micro-domains were well identified. Looped (triple arrow), bent (double arrow), and linear (single arrow) shaped domains appeared independently as a basic structural unit in the transverse alignment. The micro-domains were clearly identified as components of domains under the TEM. The dimensions of domains in Fig. 10 agreed well with those under the SEM. Moiré fringes were detected in most graphitized carbon sheets (double arrow).

Many voids which were classified as meso- (single dotted arrow) and micro-voids (double dotted arrow) were also detected in the transverse sections. Such micro- (around 5 nm) and meso-voids (10–40 nm) were not observed in the stabilized fibre. The graphitic shrinkage of micro-domains and domains may leave them in thin interlocations, as illustrated in Fig. 11,

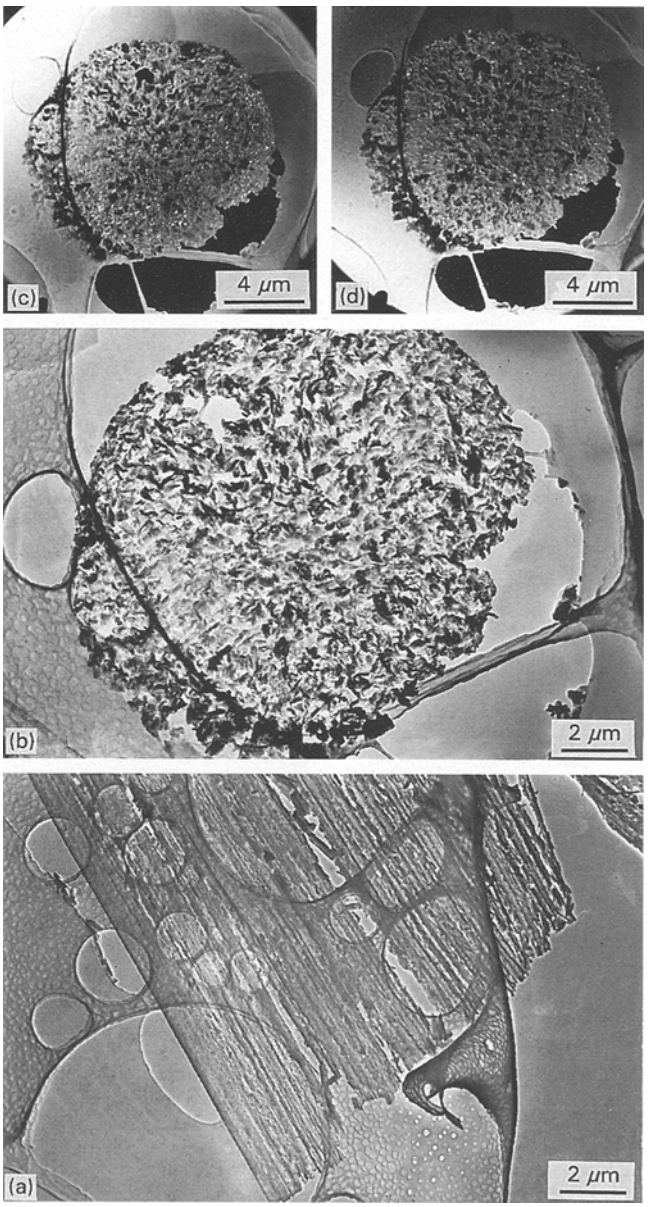

Figure 8 TEM images of graphitized fibre spun at 295 °C. (a) TEM bright-field image of the longitudinal section, (b) TEM bright-field image of the transverse-section. (c, d) Corresponding TEM orthogonal 0 0 2 dark-field images of (b).

although the macro-scale shrinkage leading to the smaller diameter of the fibre certainly took place. Fig. 12 exhibits a lattice fringe image of the transverse section in the graphitized fibre. The micro-domain was observed densely to be composed of one or several cluster units in the case of the graphitized fibre. The continuity of the micro-domains should be noted at the bent point. Inside each linear part, stacking of straight carbon planes was well organized. The linear parts in Fig. 11 were 30 nm long and 8 nm thick, corresponding to those of micro-domain units in Fig. 10. In particular, the bent parts of micro-domains formed the walls of micro-voids, P in Fig. 11. Smaller layer stacks were also observed in Fig. 11, carrying smaller porosity.

Fig. 12 shows the bright-field image of the longitudinal section of the graphitized fibre. The electron diffraction pattern shows a 0 0 6 reflection, indicating the excellent alignment of carbon layers along the fibre axis. Five elongated fibrils are easily recognized in this photograph. A fibril marked with a single arrow was 200 nm thick. Such thickness is very reasonable, corresponding to the transverse dimension of domains. Some parts were well graphitized with characteristic Moiré fringes (double arrow). Between fibrils (i.e. between domains), some vacant zones (meso-voids) around 30 nm appeared.

More careful observation of the inner part of one fibril showed that the micro-domain unit was composed of one or several clusters, being arranged in a smoothly undulating manner along the fibre axis. The dimensions of micro-domains in the longitudinal sections ranged around 100 nm in length and 10–40 nm in thickness as observed in Fig. 13 (a higher magnification image of Fig. 12). Such dimensions of micro-domains agreed well with those found by SEM (Fig. 7b). These micro-domains piled up to form a fibril unit along the fibre axis. Micro-domains of small

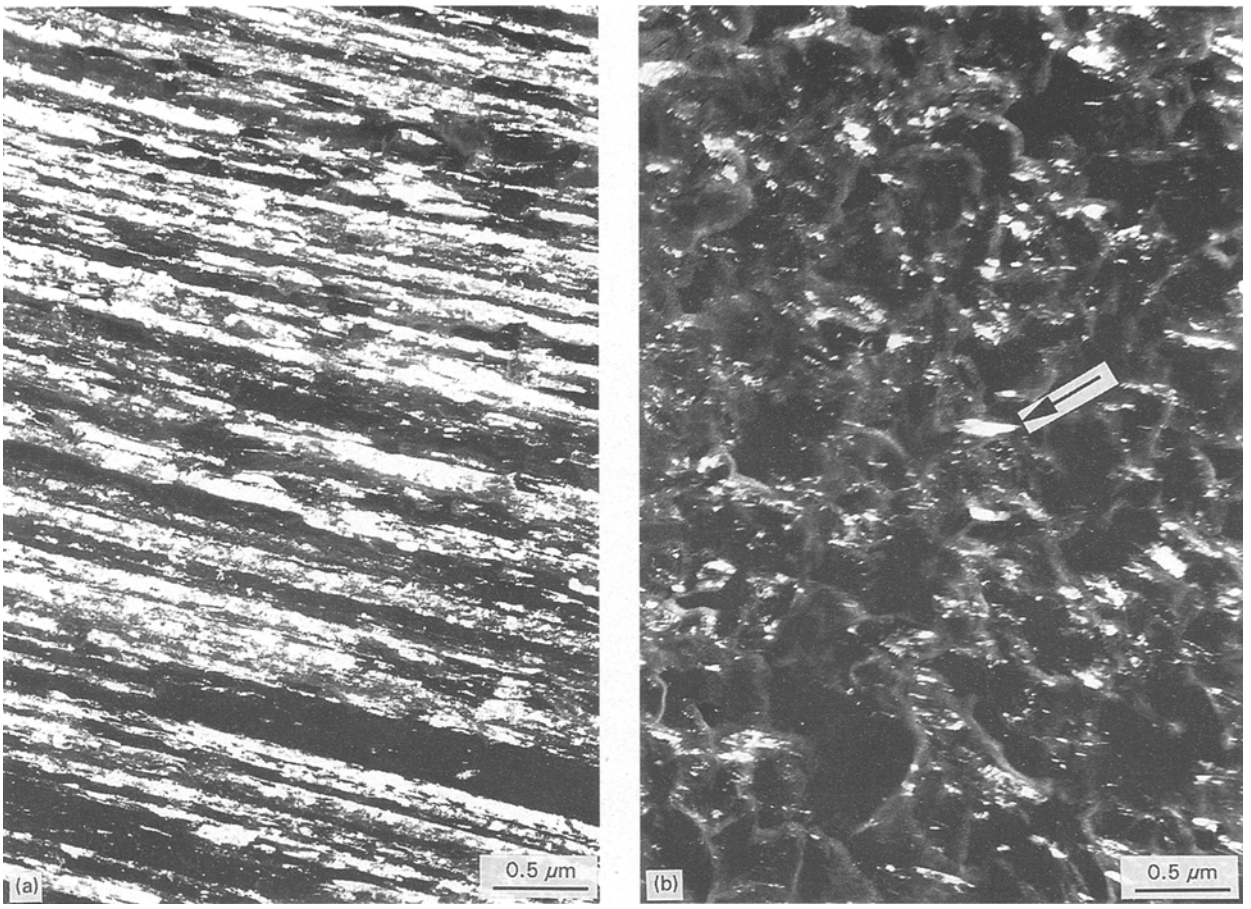

Figure 9 TEM 0 0 2 dark-field images of the graphitized fibre spun at 295 °C. (a) Longitudinal section; (b) transverse section.

scale, which were piled up more or less perfectly along the fibre axis, resulted in the formation of the micro-voids by intra-domain shrinkage (dotted arrow), as shown in Fig. 14. The average size of micro-voids was around 5 nm, observed as illustrated by P in the figure.

3.3. Change of transverse shape and alignment in the mesophase pitch-based carbon fibre according to spinning

Methylnaphthalene pitch was spun through a Y-shaped die hole at 275, 285 and 295 °C. Above 285 °C spinning temperature, the transverse shape of the fibres changed from triangular to round [17].

Fig. 15 shows scanning electron micrographs of the carbonized fibres. The trilobal shape of the fibre in Fig. 15a exhibited a radial alignment more developed in the outer area, but rather random alignment in the inner part. Such a radial trend reduced gradually with higher spinning temperature, accompanied by a change in transverse shape to round. At 295 °C spinning temperature, the round-shaped transverse section of fibre with random alignment was obtained (Fig. 15c).

Fig. 15d–f show optical micrographs of the transverse sections of the stabilized fibres which were spun at 275, 285 and 295 °C, respectively. Neither macro-voids nor cracks, which were often observed in the fibres from the same pitch spun through a round-shaped spinning die hole [25], were observed in these fibres. Fig. 15d shows a well-developed skin–radial alignment of the trilobal-shaped fibre spun at 275 °C. In each lobe, the colours are brighter in the skin area. For a given position on the rotating stage of the microscope, the two parallel flat edges of one lobe appeared yellow, while the top of the lobe appeared blue. The alignment in the inner part was not well defined by OM, as often recognized with a random alignment. At 285 °C, the skin–radial zone tended to spread into the inner area (Fig. 15e) together with a change of the transverse shape, although the skin–radial alignment was moderated. At 295 °C, the alignment changed to more or less random, showing a mixture of mosaics in certain sections (Fig. 15f).

Fig. 15g and h, i and j, and k and l show the TEM 0 0 2 dark-field images of ultra-thin transverse-sections of stabilized fibres taken at two orthogonal positions of the objective aperture on the 0 0 2 ring. The corresponding orientation of aromatic layers selected by the aperture is indicated in the photographs by a double bar. In Fig. 15g, the flat edges in the lobe of the transverse section located at the bottom left of the photograph appeared dark. In contrast, the inner part of the lobe (parallel to the flat edges) and the top of the lobe were bright. Fig. 15h

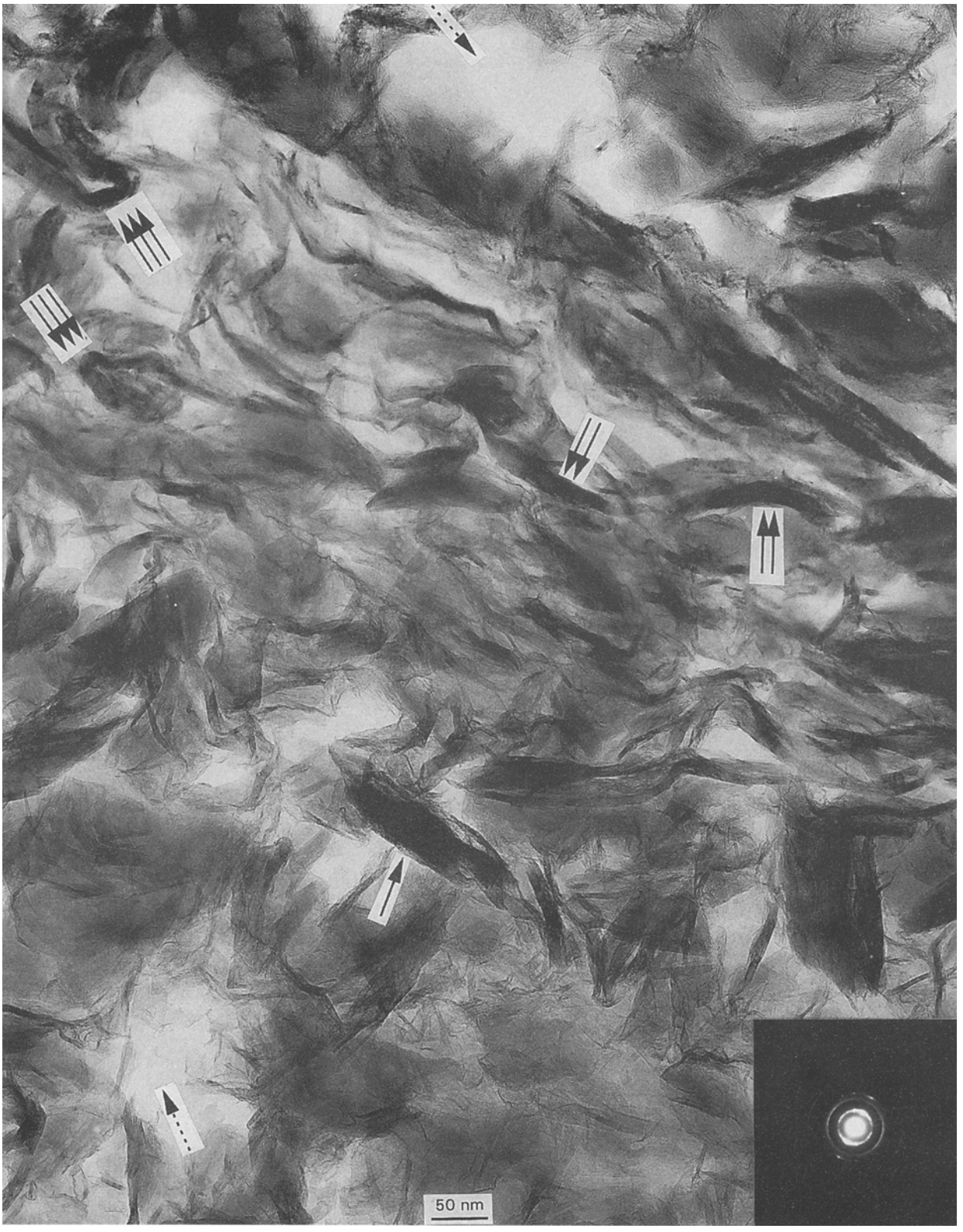

Figure 10 High-magnification TEM bright-field image of the transverse section in the graphitized fibre spun at 295 °C.

shows that the flat edges which were dark in Fig. 15g became bright, whereas the top of the lobe and the central part became dark by displacing the aperture by 90°. These two observations confirm the skin–radial alignment of the transverse section of the fibre spun at 275 °C. In the central area of each lobe, the aromatic layers are preferentially aligned parallel to the flat edges of the lobe. The distinct regularity in the bright areas was no longer observed from the skin to the centre of the transverse section in the fibre spun at 285 °C (Fig. 15i and j). Random alignment was introduced in the fibre. Fig. 15k and l show a homogeneous distribution of bright domains in the fibre spun at 295 °C. This confirms the random character of its alignment in the round-shaped transverse section.

Figure 11 TEM lattice fringe image of the transverse section of the graphitized fibre spun at 295 °C.

3.4. Crystallographic parameters and mechanical properties of the resultant fibres

Fig. 16 shows the degree of preferred orientation (DO(%)) of as-spun, stabilized, carbonized and graphitized fibres which were spun through both Y-shaped and round die holes at a spinning temperature of 295 °C. Fibres spun through a Y-shaped die hole exhibited a higher degree of orientation than those spun through the round die hole, by heat treatment up to 150 °C. However, further heat treatment up to 2500 °C provided a slightly higher degree of orientation to the fibres spun through round die hole.

Figure 12 High-magnification TEM bright-field image of the longitudinal section in the graphitized fibre spun at 295 °C.

$L_{c(0\,0\,2)}$ values of fibres spun at 295 °C through a Y-shaped die hole and round die holes were 23 and 21 nm, respectively.

Mechanical properties of graphitized fibres are summarized in Table III. Excellent mechanical properties were obtained with fibres spun through a Y-shaped die hole. A higher spinning temperature provided better mechanical properties. The graphitized round fibre (diameter ~9 μm) spun at 295 °C through the Y-shaped die hole, showed strain to break, tensile strength, modulus and compressive strength as high as 0.47%, 410 kg mm^{-2}, 87 ton mm^{-2}, and 70 kg mm^{-2}, respectively, while the graphitized fibre spun through the round die hole (diameter ~7 μm) had 0.38%,

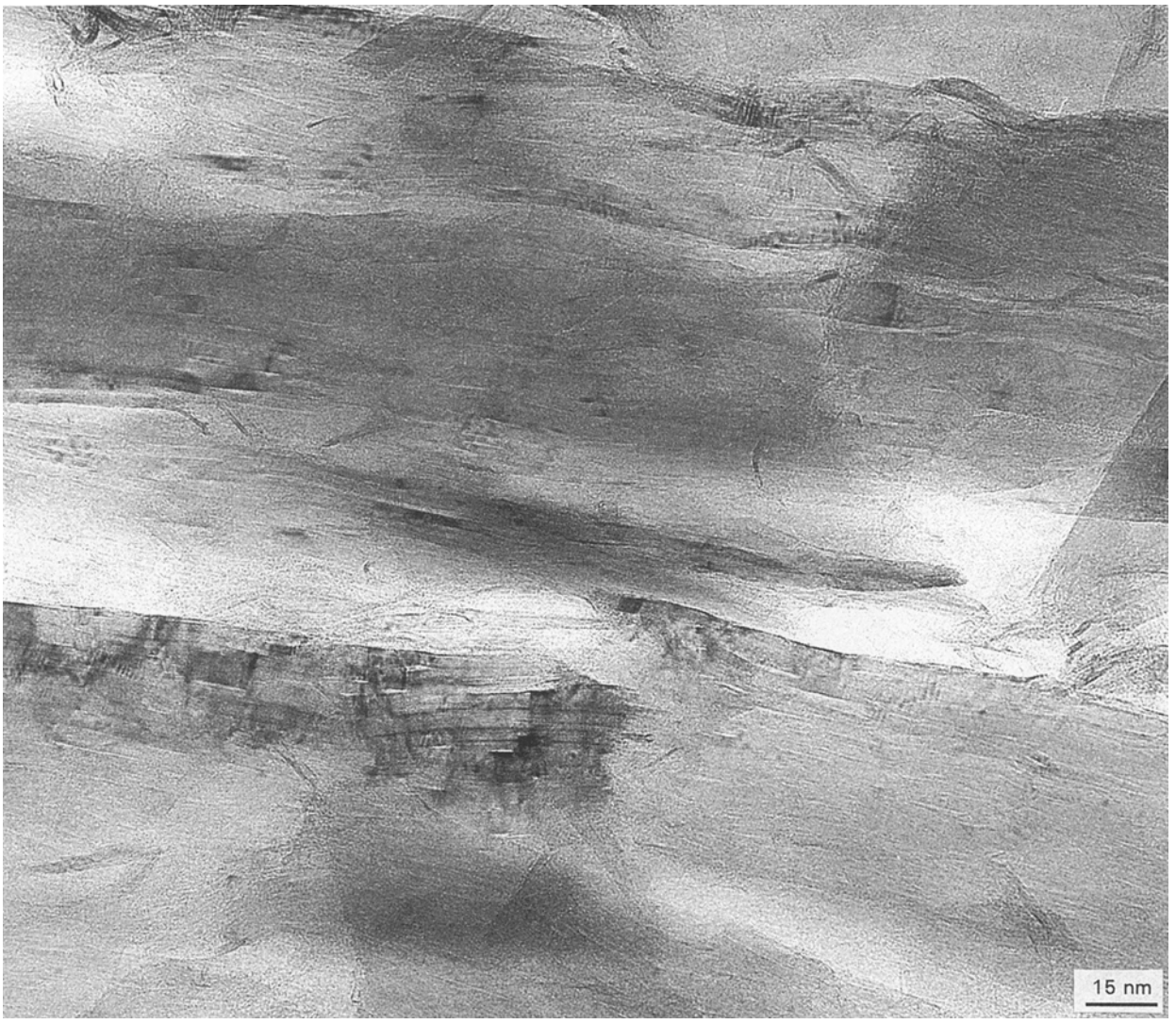

Figure 13 Higher magnification photograph of Fig. 12.

288 kg mm^{-2}, 72 ton mm^{-2}, and 60 kg mm^{-2}, respectively. The better performances of fibres spun through the Y-shaped die hole are very obvious.

4. Discussion

The present study shows that the higher performance, especially the remarkable tensile and compressive strengths, of the methylnapthalene-derived mesophase pitch-based round-shaped carbon fibre spun through a Y-shaped spinning die hole at 295 °C may be ascribed to its random alignment in the transverse section under OM, SEM, and TEM.

OM shows the random distribution of rather spherical isochromatic spots of around 0.5 μm diameter. However, SEM shows that the fibre consists of domains of various shapes, the length and thickness of which were above and under 100 μm, respectively. Their shapes can be represented as linear, bent, multibent, and looped shapes. Such domains of various shapes are randomly distributed in the transverse section although several pieces of linear domains gather to form layers which are irregularly distributed. The respective domains consist of micro-domains, around 10–100 nm long and 1–100 nm thick respectively. Such micro-domains are found by high-resolution SEM to consist of one or several units of graphitic layers in the graphitized fibre, as revealed by TEM. Several pieces of micro-domains are aligned in the same orientation to form a whole domain, or its part, when the shape of domain is bent or looped. The micro-domain is basically a graphitic unit where the hexagonal planes are stacked by $\sim$ 30 nm in length and $\sim$ 8 nm height. Such dimensions of the graphitic cluster determined by X-ray diffraction were certainly smaller than those obtained by X-ray diffraction. Some graphitic units are located in much the same direction, probably giving the larger values in the X-ray diffraction.

A number of voids are observed in the transverse section at the inter-domains (between domains) and intra-domain (between micro-domains) locations. The microscopic random alignment suffers from certainly fewer voids of such categories.

The microscopic randomness of domain distribution increases the tensile and compressive strengths

Figure 14 TEM lattice fringe image of the longitudinal section in the graphitized fibre spun at 295 °C.

through moderating the concentration of stress at one point. Fewer voids also increase the strength per unit transverse area.

Spinning at a lower temperature of 270 °C produces a trilobal-shaped fibre where the domains are aligned radial in the skin, random in the intermediate area and lined-up at the centre as shown in Fig. 17b. Such a line symmetry alignment has been reported in the thin slit-shaped fibre, and is termed the symmetry double layer with radial edge (SDL). The thin space between the nozzle walls appears to produce such a unique alignment at the lower spinning temperature where the shape and alignment induced in the nozzle are stored in the fibre. The domains are dominant ranging over 100 nm in length.

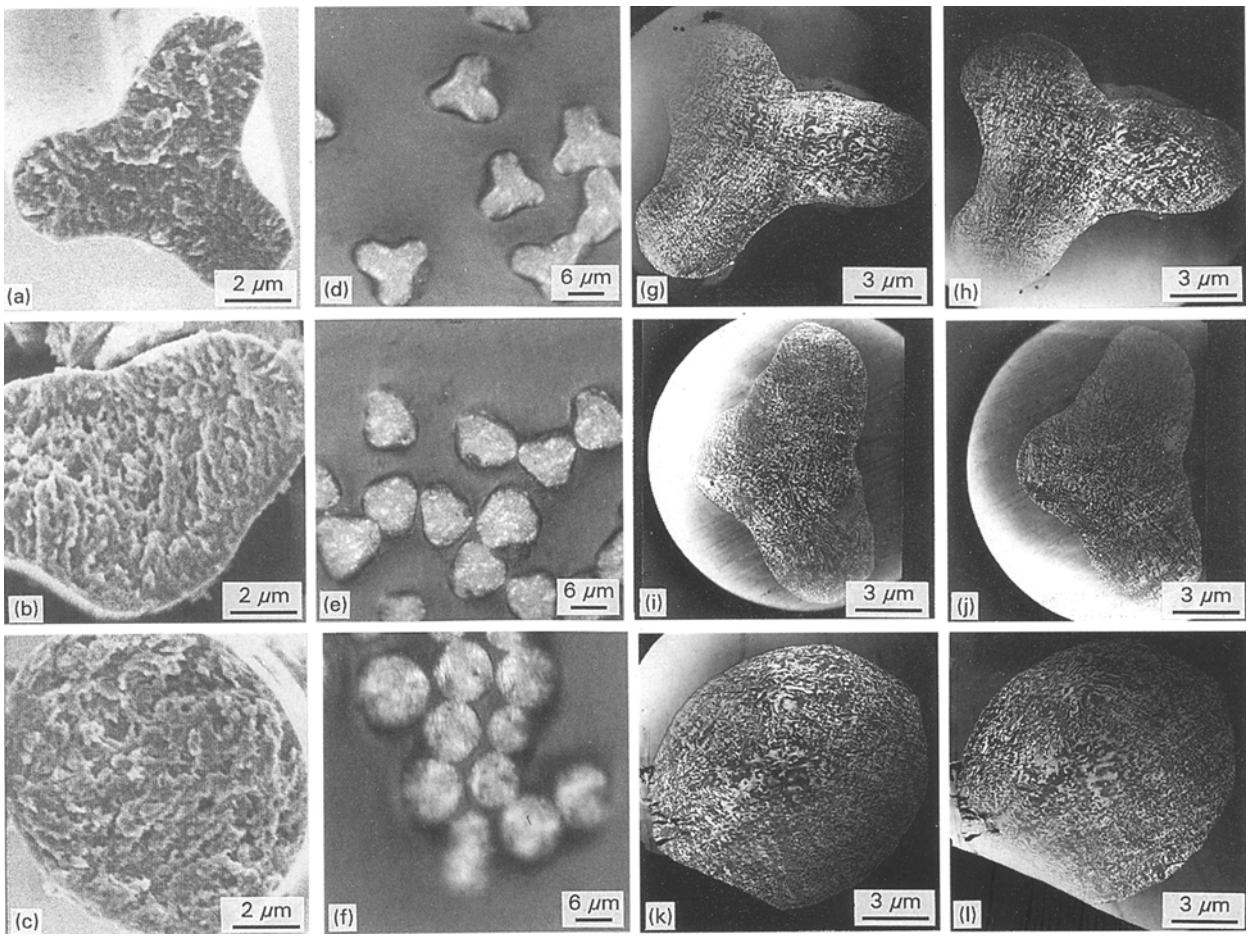

Figure 15 (a – c) Scanning electron micrographs of transverse sections of carbonized fibres spun at 275, 285 and 295 °C, respectively. (d–f) Optical micrographs of transverse sections of stabilized fibres spun at 275, 285 and 295 °C, respectively. (g–l) TEM orthogonal 0 0 2 dark-field images of ultra-thin transverse sections of stabilized fibres spun at (g, h) 275, (i, j) 285 and (k, l) 295 °C, respectively.

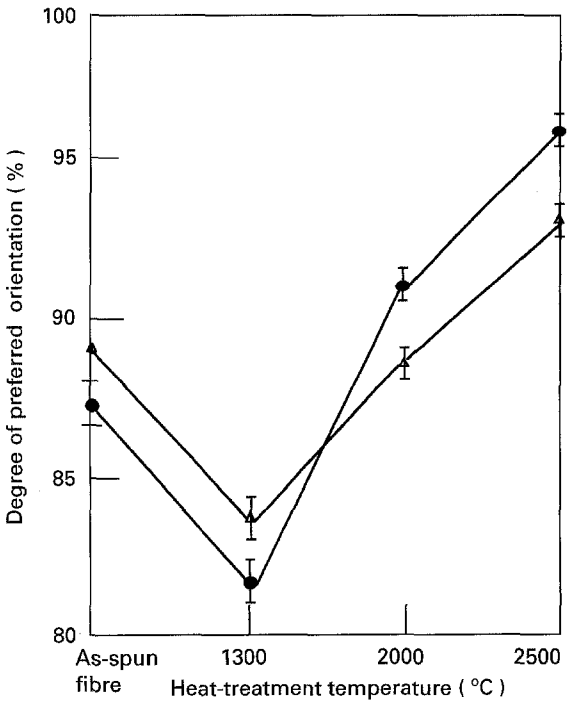

Figure 16 Degree of preferred orientation, DO(%), of fibres. (●) Fibre spun through a round-shaped spinning die hole, (△) fibre spun through a Y-shaped spinning die hole.

A slightly higher spinning temperature of 285 °C deformed the shape to triangular and the radial alignment became diverse in the outer area. The bent shape of the domains is dominant.

At a higher spinning temperature, 295 °C, a dramatic change of domain shape occurred. All domains which are bent or looped are distributed homogeneously in the transverse section, showing almost complete random alignment. No linear shape of the domain is observed. Fig. 18 shows schematic pictures of the transverse alignments in the fibre spun through a Y-shaped spinning die hole at 275, 285 and 295 °C.

In the longitudinal section of the fibre, the isochromatic stripes (fibrils) run infinitely parallel to the fibre axis under the polarized optical microscope. Such an isochromatic stripe may agree with the fibril which was observed under the SEM. The width of the fibril reflects the transverse shape and dimensions of domains running parallel. Some meso-voids are observable in the TEM bright-field image, although quantitative comparison was not attempted in the present study.

The stabilized fibre appears to exhibit basically the same alignment under the polarized microscope as that of the graphitized fibre. Domains are more closely

TABLE III Mechanical properties of graphitized fibres

Nozzle	Spinning temp. (°C)	Shape of fibre	Texture	Diameter (μm)	Area (μm^2)	Δl^a (%)	DO[b] (%)	L_c (nm)	δ_t^c ($kg\,mm^{-2}$)	E_t^d ($ton\,mm^{-2}$)	δ_c^e ($kg\,mm^{-2}$)
Circular	295	Circular	On-Rd[f]	7.0	38	0.38	95.4	21	288	72	60
Y	275	Trilobal	Ra[g]	–	64	0.45	93.8	21	330	72	–
	285	Triangle	Ra-Rd[h]	–	42	0.45	94.2	29	360	80	61
	295	Circular	Rd-On[i]	9.0	64	0.47	94.2	23	410	87	70

[a]Strain to break. [b]Degree of preferred orientation. [c]Tensile strength. [d]Young's modulus. [e]Compressive strength (composite method: $V_f = 60$ vol %). [f]Onion-random. [g]Radial. [h]Radial–random. [i]Random–onion

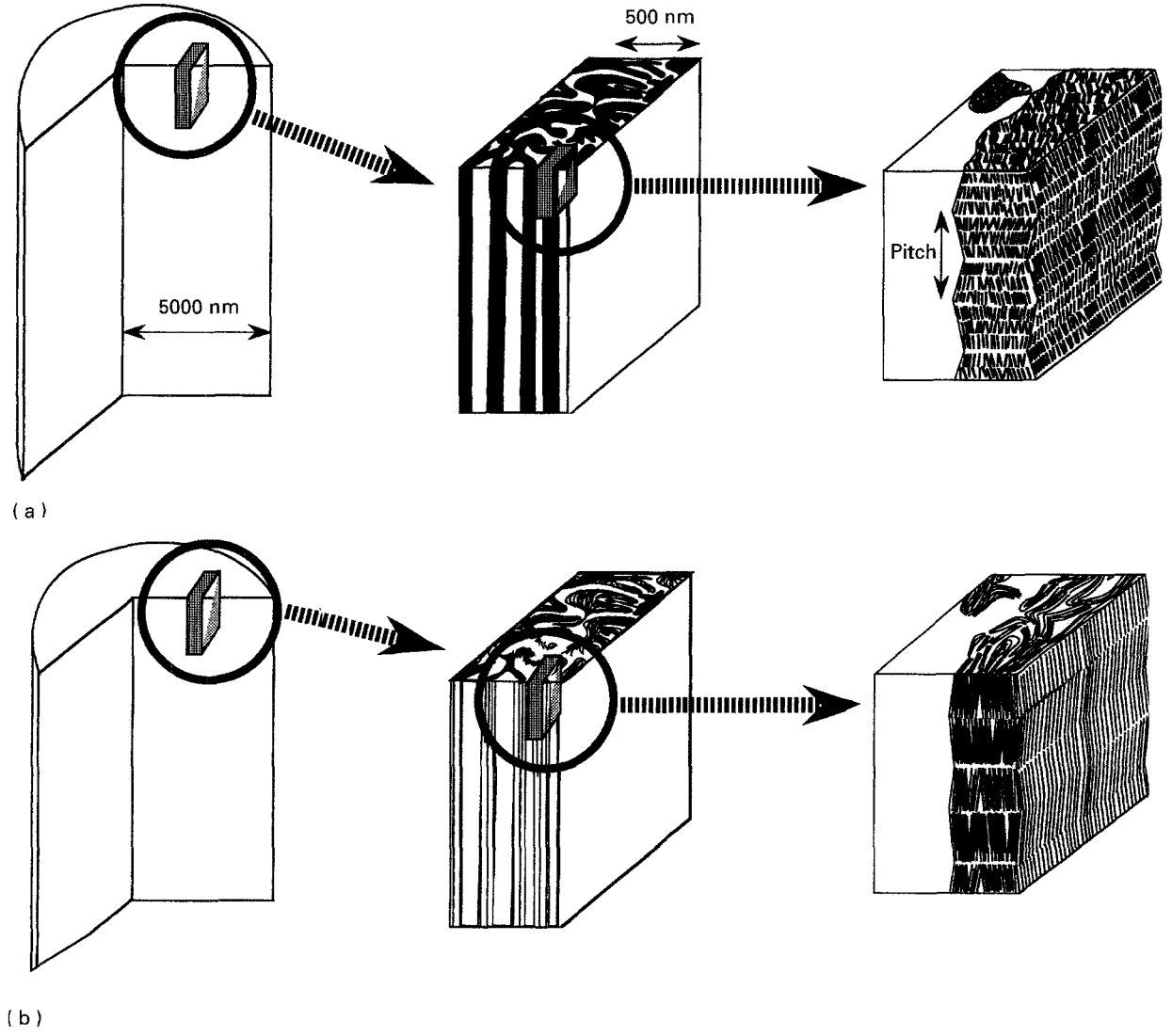

Figure 17 Schematic pictures of the structures in the (a) stabilized and (b) graphitized pitch-based fibre.

packed in the fibre, their shapes being very similar. However, the dimensions, especially their thickness, appear larger in the stabilized fibre. The shrinkage due to the carbonization and graphitization takes place to reduce the dimension of the domains, inducing voids in the fibre.

No micro-domains were observed in the stabilized fibre under TEM because of the limited size of aromatic planes. However, the TEM lattice fringe image indicated some stacking units of aromatic planes and their approximate orientation (see Fig. 2). A few domains of linear shape but mostly bent and looped shapes were revealed in the TEM bright-field images. It should be pointed out that the dimensions of aromatic clusters and micro-domains are very different in the stabilized fibre, indicating the carbonization and graphitization allowing the growth of clusters into graphitic layers of larger dimensions within the micro-domain.

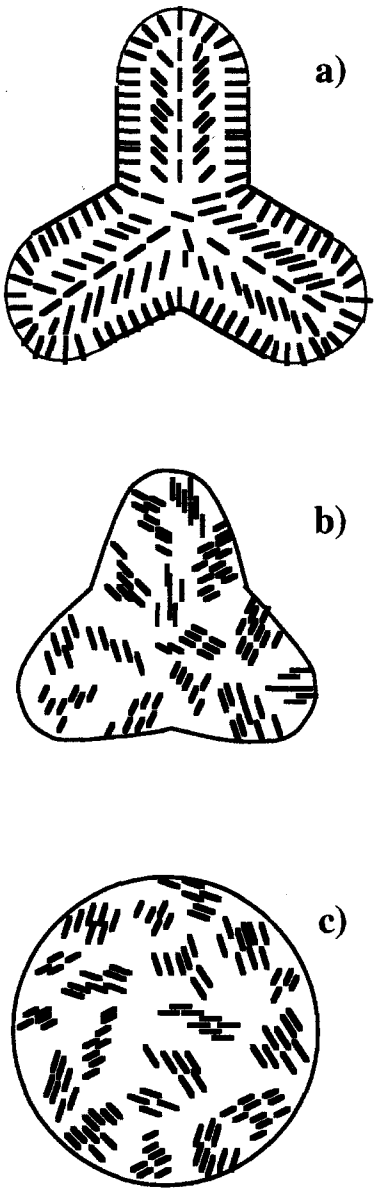

Figure 18 Models of the transverse alignments in the fibres spun through a Y-shaped spinning die hole at (a) 275 °C, (b) 285 °C, and (c) 295 °C.

The longitudinal section of the stabilized fibre exhibited basically the same features under the polarized microscope as those of the graphitized fibre. The endless fibrils which resulted from the assembly of micro-domains, run parallel to the fibre axis. Such fibrils are homologous to the domains in the transverse section except for their size. No voids originating in the inter-domain shrinkage were observed in the stabilized fibre. TEM revealed the more detailed shape of such fibrils. The fibrils reflect the same brightness, indicating the same orientation of aromatic planes. A higher magnification TEM dark-field image further clarifies the shapes and alignment of domains in both sections. Elongated fibrils oriented parallel to the fibre axis appear to have no limit. The thickness of the elongated fibrils varies in a 20–200 nm range, reflecting the very complex disclinations (bent, multi-bent, and looped shapes) of the transverse alignment with domains. The length of domains in the transverse section can be evaluated to be over 100 nm.

Although the stabilized mesophase pitch fibre consists of structural units of various dimensions, only domains and clusters are defined by X-ray. No other structural units could be observed at this stage of ordering in the carbon planes. In the particular round fibre of the present study, domains are aligned randomly in irregular shapes in the transverse section, while they are elongated mutually parallel to the fibre axis in its longitudinal section.

Carbonization and graphitization change the longitudinal structure in the same manner to that in the transverse section. The only difference is that aromatic clusters, micro-domains, and graphitic layers have very large dimensions along the fibre axis and they are all aligned at least approximately parallel to the fibre axis. Higher-magnification TEM bright-field images indicate that there is certainly a slight discontinuity between the micro-domains and graphitic layers. Such a longitudinal structure again appears to depend upon the spinning conditions and resulting transverse alignment of the carbon fibre.

In the present study, the round-shaped fibre spun through a Y-shaped spinning die hole first exhibited a higher degree of preferred orientation, up to a heat-treatment temperature of 1500 °C, compared to that of a fibre spun through a round-shaped die hole, while above 1500 °C, the fibre spun through the round-shaped die hole had a higher degree of preferred orientation. The fibrils derived from the linear-shaped domains in the transverse section may be better aligned parallel to the fibre than those derived from the bent or loop-shaped domains. The higher temperature of heat treatment may allow graphitization in the former alignment. Thus, a greater number of bent and looped domains in the fibre with the random transverse alignment may be the principal reason for the low degree of preferred orientation compared to the fibre with the typical radial alignment by heat treatment above 1500 °C [26].

References

1. S. OTANI, K. OKUDA and H.S. MATSUDA, "Carbon fiber" (Kindai, Tokyo, 1983) p. 231.
2. S. OTANI and A. OYA, in "Composites '86: recent advances in Japan and United States" K. Kawata, S. Uekawa and K. Kobayashi, (Japan Society for Composite Materials, 1986) p. 1.
3. L.S. SINGER, *Fuel* **60** (1981) 839.
4. E. FITZER, *Carbon* **27** (1989) 62.
5. W. RULAND, *Appl. Polym. Symp.* **9** (1969) 293.
6. L.S. SINGER, *Carbon* **16** (1978) 409.
7. S.H. YOON, Y. KORAI and I. MOCHIDA, *ibid.* **31** (1993) 849.
8. T. HAMADA, M. FURUYAMA, Y. SAJIKI, T. TOMIOKA and M. ENDO, *J. Mater. Res.* **5** (1990) 6.
9. T. MATSUMOTO, *Pure Appl. Chem.* **57** (1985) 1553.
10. I. MOCHIDA, H. TOSHIMA, Y. KORAI and T. MATSUMOTO, *J. Mater. Sci.* **23** (1988) 670.
11. I. MOCHIDA, H. TOSHIMA, Y. KORAI and T. NAITO, *ibid.* **23** (1988) 678.
12. M. INAGAKI, N. IWASHITA, Y. HISHIYAMA, Y. KABURAGI, A. YOSHIDA, A. OBERLIN, K. LAFDI, S. BONNAMY and Y. YAMADA, *TANSO* **147** (1989) 57.

13. J.D. FITZGERALD, G.M. PENNOCK and G.H. TAYLOR, *Carbon* **29** (1989) 139.
14. A. OBERLIN, in "Chemistry and physics of carbon", Vol. 22, edited by P.A. Thrower (Dekker, New York, 1989) p. 1.
15. M. MATSUMOTO, T. IWASHITA, Y. ARAI and T. TOMIOKA, *Carbon* **31** (1993) 715.
16. I. MOCHIDA, S.H. YOON and Y. KORAI, *J. Mater. Sci.* **28** (1993) 2331.
17. *idem, ibid.* **28** (1993) 2135.
18. F. FORTIN, S.H. YOON, Y. KORAI and I. MOCHIDA, *Carbon*, in press.
19. K. LAFDI, S. BONNAMY and A. OBERLIN, *ibid.* **30** (1992) 551.
20. Y. KORAI, M. NAKAMURA, I. MOCHIDA, Y. SAKAI and S. FUJIYAMA, *ibid.* **28** (1991) 561.
21. Carbon Society of Japan, "Tanso Zairyo Jitugen Gijutsu" (Kagaku Gijutsu Tokyo, 1978) p. 46.
22. Japan Society for the Promotion of Science (JSPS), *TANSO* **36** (1963) 25.
23. Japanese Industrial Standard Committe, Japanese Industrial Standards (JIS R-7601).
24. H.M. HAWTHORNE and E. TEGHTSOONIAN, *J. Mater. Sci.* **22** (1975) 41.
25. M. MATSUMOTO, T. IWASHITA, Y. ARAI and T. TOMIOKA, *Carbon* **31** (1993) 715.
26. I. MOCHIDA, S.H. YOON, N. TAKANO, F. FORTIN, and Y. KORAI, *ibid.* in press.

Received 1 August 1994
and accepted 21 February 1995